Customer No. 22,852
Attorney Docket No. **09877.0363**

IN THE UNITED STATES PATENT AND TRADEMARK OFFICE

In re Application of:	)	
	)	
Alfredo GAMBIRASIO, *et al.*	)	
	)	
Serial No.: 10/550,463	)	Group Art Unit: 2874
	)	
Filed: September 26, 2005	)	Examiner: Omar R. Rojas
	)	
For: MICROSTRUCTURED OPTICAL FIBRE	)	Confirmation No. 4626
	)	
	)	

Commissioner for Patents
P.O. Box 1450
Alexandria, Virginia 22313-1450

Sir:

DECLARATION UNDER 37 C.F.R. § 1.132

EXHIBIT B

ELSEVIER

1 June 2002

Optics Communications 206 (2002) 333–339

OPTICS COMMUNICATIONS

www.elsevier.com/locate/optcom

Multipole analysis of hole-assisted optical fibers

Zhaoming Zhu*, Thomas G. Brown

The Institute of Optics, University of Rochester, Rochester, NY 14627, USA

Received 5 February 2002; accepted 17 April 2002

Abstract

Hole-assisted optical fibers are microstructured fibers which guide light using a conventional high-index core while using a small number of air holes in the cladding to achieve desirable dispersive and/or polarization properties of the fiber. In this paper, we analyze the characteristics of the hole-assisted fibers using the multipole method of White et al. [Opt. Lett. 26 (2001) 1660], which is a rigorous boundary value method. Such properties as dispersion and birefringence are numerically investigated for fibers with different air hole patterns and sizes. Hole-assisted optical fibers exhibit low transmission loss and easily tailorable dispersion and birefringence, and therefore, would be valuable for dispersion management applications both in linear (WDM) and nonlinear (soliton) fiber telecommunications. © 2002 Published by Elsevier Science B.V.

1. Introduction

Air–silica microstructured optical fibers (ASMFs) (also termed photonic crystal fibers or holey optical fibers) have attracted a great deal of recent interest [1–9]. ASMFs consist of an arrangement of air holes running through the entire length of the fibers. Compared to conventional optical fibers, ASMFs exhibit properties such as a wide range of single-mode operation, tailorable dispersion, and easily controllable effective mode area. ASMFs are ready to lend themselves for applications such as dispersion compensation [4–6], soliton formation [7,8] and visible continuum generation [9].

However, the high transmission loss of ASMFs is one of the problems that hinder many practical applications. The transmission loss in the 1.55 μm wavelength band has been typically as high as a few tens of dB/km. Although progresses in fabrication of low-loss holey fibers with losses of a few dB/km have been recently reported [10,11], the losses are still significantly higher than those of the conventional fibers (typically 0.2–0.5 dB/km). In recent efforts to reduce the transmission loss of ASMFs, Hasegawa et al. [12–14] proposed and fabricated "hole-assisted lightguide fibers" with losses comparable to conventional fibers. The low-loss fiber has a high index core, a low index cladding, and a few air holes surrounding the core as shown in Fig. 1. It can be treated as a conventional fiber with a few air holes introduced into the cladding, therefore, a variation lying between the conventional fiber and the holey fiber.

* Corresponding author. Tel.: +1-585-275-0232; fax: +1-585-244-4936.

E-mail address: zzhu@optics.rochester.edu (Z. Zhu).

0030-4018/02/$ - see front matter © 2002 Published by Elsevier Science B.V.
PII: S0030-4018(02)01497-9

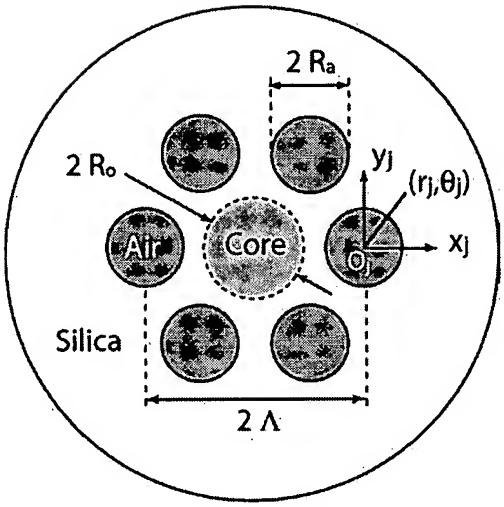

Fig. 1. Schematic of the air-hole-assisted optical fiber. The high-index core of radius R_0 is surrounded by N ($N = 6$ shown) circular air holes.

The optical properties of ASMFs have been modeled by a number of methods including both approximate methods such as the effective index method [1,15] and rigorous methods such as plane-wave-method [16,17], localized-function method [18,19], finite element method [20]. All these rigorous approaches start from the transverse field component and solve for propagation constant β and associated modal fields. For example, the localized-function method expands the transverse electric or magnetic field in terms of a Hermite–Gauss basis and solves the resultant algebraic eigenvalue equation for β. Recently, multipole method has been used in modeling the confinement loss of ASMFs ([22] and references therein), in which the EM properties of ASMFs are obtained by starting from the longitudinal field components and solving a boundary value problem. Hasegawa et al. [13] have used the full-vector finite element method to model the air-assisted fiber. In this paper, we use the multipole method to investigate the optical properties of the air-hole-assisted fiber.

In Section 2, the formation of the multipole method is reviewed. In Section 3, the effective index, group dispersion and birefringence of the fundamental mode are presented for fibers with different air hole number and size. Comparisons are also made between the air-assisted fiber and the conventional fiber and between the multipole method and the localized-function method.

2. Formulation

The multipole method starts from the longitudinal field components E_z and H_z instead of the transverse field components, just like in the case of conventional optical fibers. The longitudinal field satisfies the Helmholtz equation

$$\nabla_t^2 \begin{pmatrix} E_z \\ H_z \end{pmatrix} + (k^2 n^2 - \beta^2) \begin{pmatrix} E_z \\ H_z \end{pmatrix} = 0, \tag{1}$$

where β is the propagation constant in z direction, and $n = n(x,y)$ is the transverse refractive index profile of the fiber. The longitudinal field components determine the transverse components from Maxwell's equations:

$$\mathbf{E}_t = \frac{\mathrm{i}\beta}{k^2 n^2 - \beta^2} \left(\nabla_t \mathbf{E}_z - Z_0 \frac{k}{\beta} \hat{z} \times \nabla_t \mathbf{H}_z \right), \tag{2}$$

$$\mathbf{H}_t = \frac{\mathrm{i}\beta}{k^2 n^2 - \beta^2} \left(\nabla_t \mathbf{H}_z + \frac{k}{Z_0 \beta} \hat{z} \times \nabla_t \mathbf{E}_z \right), \tag{3}$$

where $Z_0 = \sqrt{\mu_0/\varepsilon_0}$ is the impedance of free space.

From the boundary conditions at all the interfaces (i.e., the continuity of tangential components of electric and magnetic fields), we can solve for the propagation constant β and corresponding fields.

We consider the fiber with a high-index guiding core and N circular air holes as illustrated in Fig. 1. The high-index core has refractive index n_0 and radius R_0. The jth air hole has index of unity and radius R_j. The cladding has refractive index $n_c (n_c < n_0)$ and it is assumed to be infinite.Within each circular region, the E_z, H_z are expressed in the form

$$E_{zj} = \sum_{m=-\infty}^{\infty} A_m^{(j)} F_m^{(j)}(p_j r_j) \exp(\mathrm{i}m\theta_j), \tag{4a}$$

$$H_{zj} = Z_0^{-1} \sum_{m=-\infty}^{\infty} B_m^{(j)} F_m^{(j)}(p_j r_j) \exp(\mathrm{i}m\theta_j), \tag{4b}$$

where

$$F_m^{(j)}(p_j r_j) = \begin{cases} J_m\left(r_0\sqrt{k^2 n_0^2 - \beta^2}\right), & j = 0 \\ I_m\left(r_j\sqrt{\beta^2 - k^2 n_j^2}\right) & \text{otherwise,} \end{cases} \tag{5}$$

and (r_j, θ_j) is the local polar coordinate with the jth circular region.

In the cladding, the longitudinal field components have the form

$$E_{zc} = \sum_{l=0}^{N}\sum_{m=-\infty}^{\infty} C_m^{(l)} K_m(q_c r_l)\exp(\mathrm{i}m\theta_l), \tag{6a}$$

$$H_{zc} = Z_0^{-1}\sum_{l=0}^{N}\sum_{m=-\infty}^{\infty} D_m^{(l)} K_m(q_c r_l)\exp(\mathrm{i}m\theta_l), \tag{6b}$$

where $q_c = \sqrt{\beta^2 - k^2 n_c^2}$.

In the above expressions, the multiple coordinate systems associated with each circular region are used. Using the addition theorem for Bessel function K_m [22], we can rewrite the E_{zc} and H_{zc} in the jth coordinate system by

$$E_{zc} = \sum_{m=-\infty}^{\infty}\left[U_m^{(j)} I_m(q_c r_j) + C_m^{(j)} K_m(q_c r_j)\right]\exp(\mathrm{i}m\theta_j), \tag{7a}$$

$$H_{zc} = Z_0^{-1}\sum_{m=-\infty}^{\infty}\left[V_m^{(j)} I_m(q_c r_j) + D_m^{(j)} K_m(q_c r_j)\right]\exp(\mathrm{i}m\theta_j), \tag{7b}$$

with

$$U_m^{(j)} = \sum_{l\neq j}\sum_{q=-\infty}^{\infty} C_q^{(l)}(-1)^q K_{m-q}(q_c r_j^l)\exp\left[\mathrm{i}(q-m)\theta_j^l\right], \tag{8a}$$

$$V_m^{(j)} = \sum_{l\neq j}\sum_{q=-\infty}^{\infty} D_q^{(l)}(-1)^q K_{m-q}(q_c r_j^l)\exp\left[\mathrm{i}(q-m)\theta_j^l\right], \tag{8b}$$

where (r_j^l, θ_j^l) is the polar coordinate of the lth origin in the jth polar coordinate system.

From the longitudinal field components, we can get the transverse tangential components using Eqs. (2) and (3)

$$E_{\theta_j} = \frac{\mathrm{i}}{k^2 n_j^2 - \beta^2}\sum_{m=-\infty}^{\infty}\left[\frac{\beta}{r_j}(\mathrm{i}m)A_m^{(j)} F_m^{(j)}(p_j r_j) - kp_j B_m^{(j)} F_m'^{(j)}(p_j r_j)\right]\exp(\mathrm{i}m\theta_j), \tag{9a}$$

$$H_{\theta_j} = \frac{\mathrm{i}Z_0^{-1}}{k^2 n_j^2 - \beta^2}\sum_{m=-\infty}^{\infty}\left[kn_j^2 p_j A_m^{(j)} F_m'^{(j)}(p_j r_j) + \frac{\beta}{r_j}(\mathrm{i}m)B_m^{(j)} F_m^{(j)}(p_j r_j)\right]\exp(\mathrm{i}m\theta_j), \tag{9b}$$

$$E_{\theta c} = \frac{\mathrm{i}}{k^2 n_c^2 - \beta^2}\sum_{m=-\infty}^{\infty}\left\{\frac{\beta}{r_j}(\mathrm{i}m)\left[U_m^{(j)} I_m(q_c r_j) + C_m^{(j)} K_m(q_c r_j)\right] - kq_c\left[V_m^{(j)} I_m'(q_c r_j) + D_m^{(j)} K_m'(q_c r_j)\right]\right\}\exp(\mathrm{i}m\theta_j), \tag{9c}$$

$$H_{\theta c} = \frac{\mathrm{i}Z_0^{-1}}{k^2 n_c^2 - \beta^2}\sum_{m=-\infty}^{\infty}\left\{kn_c^2 q_c\left[U_m^{(j)} I_m'(q_c r_j) + C_m^{(j)} K_m'(q_c r_j)\right] + \frac{\beta}{r_j}(\mathrm{i}m)\left[V_m^{(j)} I_m(q_c r_j) + D_m^{(j)} K_m(q_c r_j)\right]\right\}\exp(\mathrm{i}m\theta_j). \tag{9d}$$

Applying Eqs. (4a)–(9d) to the boundary conditions at all the $N+1$ circular interfaces, we obtain an infinite system of linear equation in terms of the unknown coefficients $C_m^{(j)}$ and $D_m^{(j)}$ $(j = 0, 1, \ldots, N)$. It can be written in a matrix form as

$$\mathbf{MC} = \mathbf{0}, \tag{10}$$

where $\mathbf{C}$ is the vector composing of unknown constants $C_m^{(j)}$ and $D_m^{(j)}$, and $\mathbf{M}$ is the coefficient matrix whose determinant vanishes for a nontrivial solution of $\mathbf{C}$. In order to numerically calculate the propagation constant β of the guided modes, we truncate $\mathbf{M}$ into a finite square matrix. If we limit m in the range from $-L$ to L, then the dimension of the resultant matrix is $2(N+1)(2L+1) \times 2(N+1)(2L+1)$. The propagation constants of guided modes are then obtained by iteratively scanning for dips of the determinant of the truncated matrix $\mathbf{M}$ while β/k is varied from to n_c to n_0.

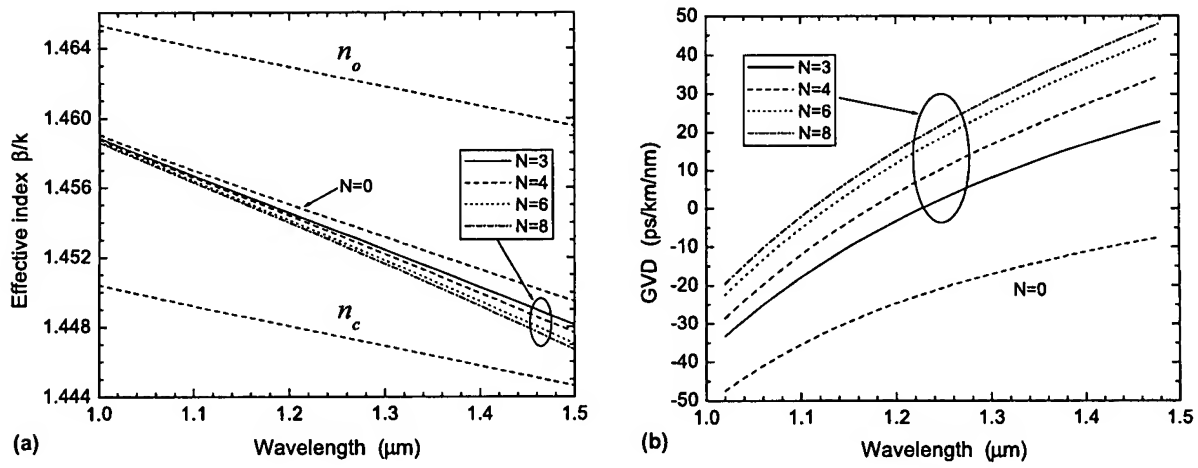

Fig. 2. Calculated (a) effective index and (b) group velocity dispersion (GVD) for air-assisted fibers with different number of identical air holes symmetrically surrounding the core. The core is doped with 10% mol GeO_2 and has a radius R_0 of 2 μm. The core-to-hole spacing Λ is 5 μm. Air holes have a radius R_a of 2 μm.

3. Results and discussion

We first consider the microstructured optical fiber as illustrated in Fig. 1. The central core is GeO_2 doped silica and is symmetrically surrounded by identical air holes in the pure silica cladding. It has fewer air holes than other ASMFs since the higher index core can efficiently confine light and thus enables low-loss propagation. When the air holes are small or far from the core, the fiber behaves like a conventional fiber. However, the air holes will significantly alter the dispersion of the fiber, especially when they are large or close to the core.

In Fig. 2, we show the calculated propagation constants and group velocity dispersions (GVD) of the fundamental guided modes in the fibers with 3, 4, 6, and 8 identical air holes. The corresponding conventional fiber ($N = 0$) is also shown for comparison purpose. It can be seen that the presence of air holes shifts the zero dispersion wavelength λ_D to shorter wavelength and that more air holes can increase anomalous dispersion in the long wavelength region. Alternatively, large air hole or being closer to the core can also increase anomalous dispersion as shown in Fig. 3.

The modal fields, Poynting vector component of the fundamental mode (x-polarized) are shown in Fig. 4 for a 6-air-hole fiber at wavelength of 1.5 μm. As can be seen, the air holes do not change the energy distribution very much; average energy flow density $\langle S_z \rangle$ is essentially the same as a conventional fiber. This feature should make the fiber easy to splice with conventional single mode fiber with little loss. However, both the propagation constant and GVD are changed significantly by the air holes.

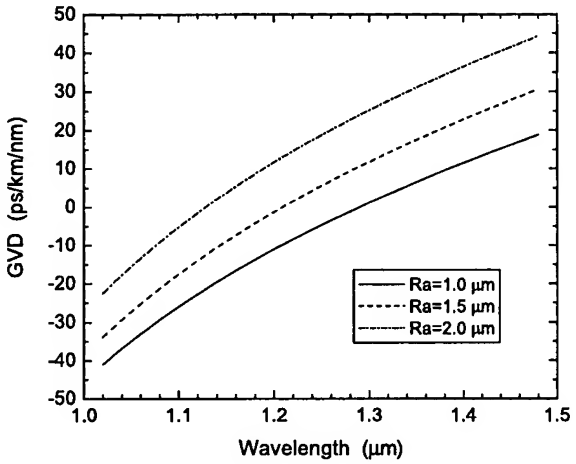

Fig. 3. Calculated GVD for 6-air-hole fibers with different air hole sizes. The core is doped with 10% mol GeO_2 and has a radius R_0 of 2 μm. The core-to-hole spacing Λ is 5 μm.

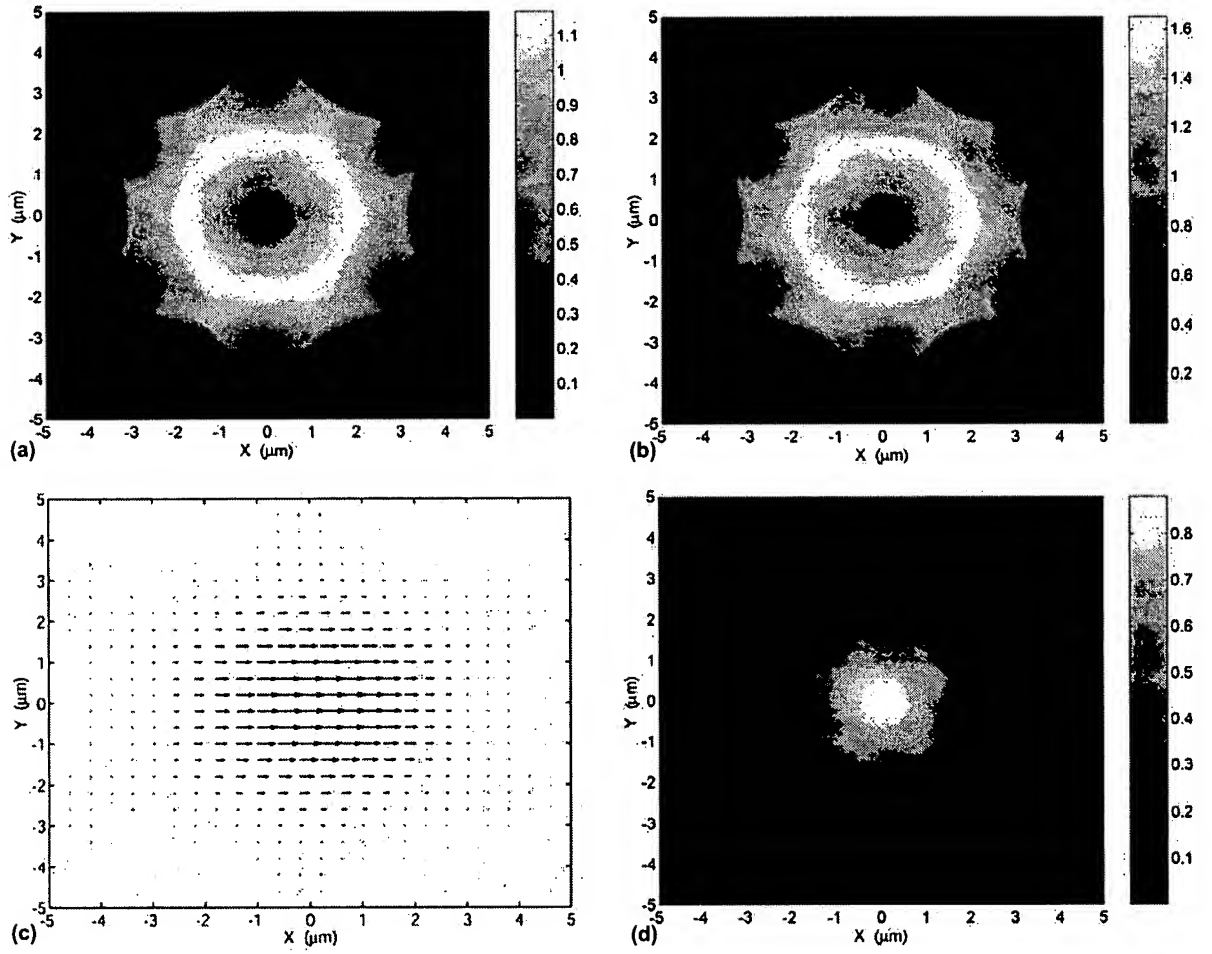

Fig. 4. (a) $|E_z|$, (b) $|H_z|$, (c) $\vec{E}_t$, and (d) $\langle S_z \rangle$ for the fundamental mode (x-polarized) of a 6-air-hole fiber at wavelength of 1.5 μm (core radius $R_0 = 2$ μm; 10% mol GeO_2 doping in the core; air hole radius $R_a = 2$ μm; hole-hole spacing $\Lambda = 5$ μm).

The fiber can be made to be polarization maintaining by inducing high birefringence through changing either the position or size of some of the air holes. As an example, here we consider changing the size of some air holes as illustrated in Fig. 5(a). In Fig. 5(b), we show the calculated birefringence B when the radius R_b of the two opposite air holes is varied.

We notice that, for long wavelengths, the effective index of the fundamental mode cannot be found via the searching technique mentioned in Section 2, because the modal fields extend more significantly into the air hole the effective index of the mode β/k is smaller than n_c. In this limit, β is complex and the guided mode becomes lossy. However, the multipole method is still capable of solving the problem by using more general formulations and proper boundary conditions as in [21]. As an alternative, we use the localized-function method [18,19] for the long wavelengths. We show the results from both methods in Fig. 6. They agree very well, especially in the short wavelength region.

The multipole method verifies the degeneracy of the fundamental mode of the air-hole-assisted fiber with N-fold ($N \geqslant 3$) symmetry (More general

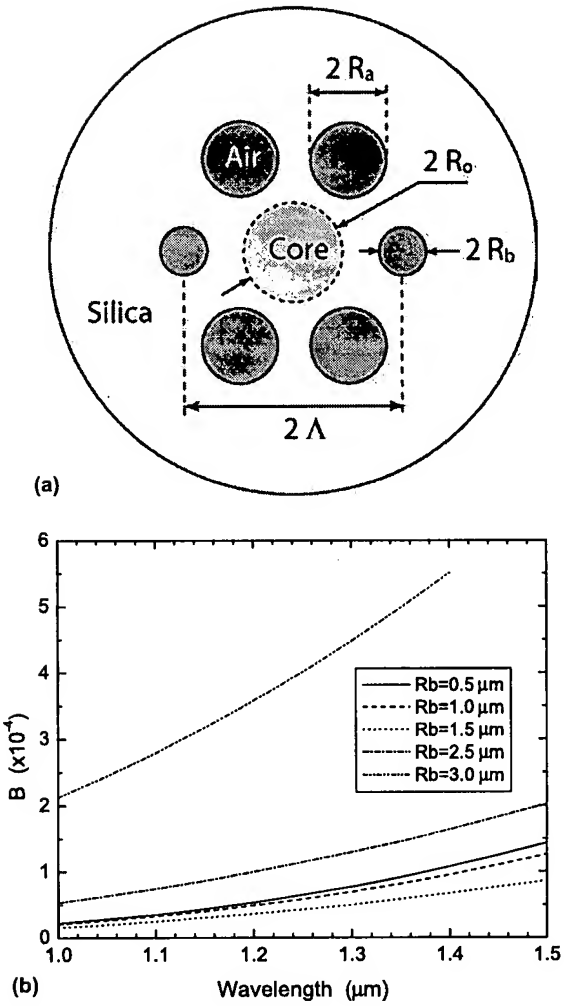

Fig. 5. Birefringence of a 6-air-hole fiber when the size of the two opposite air holes varies. (a) Schematic of the fiber considered in the calculation. R_a is fixed, and R_b varies. (b) Calculated birefringence for fibers shown in (a) with different R_b. The core is doped with 10% mol GeO_2 and has a radius R_0 of 2 μm. $R_a = 2$ μm. The core-to-hole spacing Λ is 5 μm.

discussions of the symmetry and degeneracy of microstructure optical fibers have been made in [23,24]). For a 3-fold symmetric hole-assisted fiber, in Fig. 7 we show the determinant of the matrix **M** when the effective index β/k is scanned from n_c to n_0. The presence of only one sharp dip indicates no splitting of the fundamental mode and verifies that this method introduces no numerical breaking of the degeneracy.

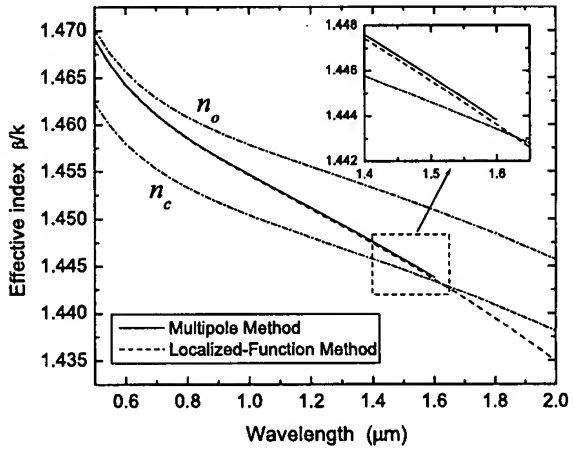

Fig. 6. Comparison between the multipole method and the localized-function method for a fiber with six symmetrically arranged identical air holes. The core is doped with 5% mol GeO_2 and has a radius R_0 of 3 μm. The core-to-hole spacing Λ is 6 μm. Air holes have a radium R_a of 2 μm.

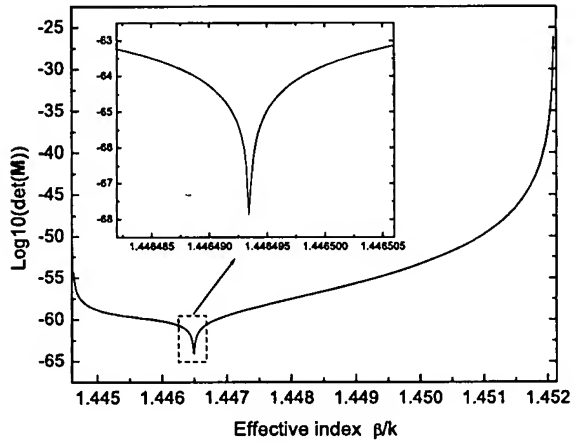

Fig. 7. The determinant of **M** vs. effective index β/k for a fiber with three symmetrically arranged identical air holes. The inset shows details around the dip. The core is doped with 5% mol GeO_2 and has a radius R_0 of 3 μm. The core-to-hole spacing Λ is 6 μm. Air holes have a radius R_a of 2 μm.

4. Conclusion

We have analyzed the guiding properties of a special type air–silica microstructured fiber that has a high-index guiding core and a single ring of air holes in the cladding, by solving a rigorous boundary value problem. The group velocity

dispersions of the fiber with different number of air holes and different air hole sizes are numerically obtained. The birefringence of the fiber by changing the air hole size is also investigated. With important features such as low transmission loss, tailorable dispersion and polarization, the air-hole-assisted optical fiber may be of great promise in lightwave applications.

References

[1] T.A. Birks, J.C. Knight, P.St.J. Russell, Opt. Lett. 22 (1997) 961–963.

[2] J.C. Knight, J. Boreng, T.A. Birks, P.St.J. Russell, Science 282 (1998) 1476–1478.

[3] R.F. Cregan, B.J. Mangan, J.C. Knight, T.A. Birks, P.St.J. Russell, P.J. Roberts, D.C. Alien, Science 285 (1999) 1537–1539.

[4] T.A. Birks, D. Mogilevtsev, J.C. Knight, P.St.J. Russell, IEEE Photon. Technol. Lett. 11 (1999) 674–676.

[5] J.C. Knight, J. Arriaga, T.A. Birks, A. Ortigosa-Blanch, W.J. Wadsworth, P.St.J. Russell, IEEE Photon. Technol. Lett. 12 (2000) 807–809.

[6] A. Ortigosa-Blanch, J.C. Knight, W.J. Wadsworth, J. Arriaga, B.J. Mangan, T.A. Birks, P.St.J. Russell, Opt. Lett. 25 (2000) 1325–1327.

[7] W.J. Wadsworth, J.C. Knight, A. Ortigosa-Blanch, J. Arriaga, E. Silverstre, P.St.J. Russell, Electron. Lett. 36 (2000) 53–55.

[8] X. Liu, C. Xu, W.H. Knox, J.K. Chandalia, B.J. Eggleton, S.G. Kosinski, R.S. Windeler, Opt. Lett. 26 (2001) 358–360.

[9] J.K. Ranka, R.S. Windeler, A.J. Stenz, Opt. Lett. 25 (2000) 25–27.

[10] H. Kubota, K. Suzuki, S. Kawanishi, M. Nakazawa, M. Tanaka, M. Fujita, CLEO2001, DPD3, 2001.

[11] J.A. West, N. Venkataramam, C.M. Smith, M.T. Gallagher, ECOC2001, Th.A.2.2, 2001.

[12] T. Hasegawa, E. Sasaoka, M. Onishi, M. Nishimura, Y. Tsuji, M. Koshiba, OFC2001, PD5, 2001.

[13] T. Hasegawa, E. Sasaoka, M. Onishi, M. Nishimura, Y. Tsuji, M. Koshiba, ECOC2001, We.L.2.5, 2001.

[14] T. Hasegawa, E. Sasaoka, M. Onishi, M. Nishimura, Y. Tsuji, M. Koshiba, Opt. Express 9 (2001) 681–686. Available from <http://www.opticsexpress.org/abstract.cfm?URI=OPEX-9-13-681>.

[15] J.C. Knight, T.A. Birks, P.St.J. Russell, J.P. De Sandro, J. Opt. Soc. Am. A 15 (1998) 748–752.

[16] A. Ferrando, E. Silvestre, J.J. Miret, P. Andres, M.V. Andres, Opt. Lett. 24 (1999) 276–278.

[17] Z. Zhu, T.G. Brown, Opt. Express 8 (2001) 547–554. Available from <http://www.opticsexpress.org/abstract.cfm?URI=OPEX-8-10-547>.

[18] D. Mogilevtsev, T.A. Birks, P.St.J. Russell, J. Lightwave Technol. 17 (1999) 2078–2081.

[19] T.M. Monro, D.J. Richardson, N.G.R. Broderick, P.J. Bennett, J. Lightwave Technol. 18 (2000) 50–56.

[20] F. Brechet, J. Marcou, D. Pagnoux, P. Roy, Opt. Fiber Technol. 6 (2000) 181–191.

[21] T.P. White, R.C. McPhedran, C.M. de Sterke, L.C. Botten, M.J. Steel, Opt. Lett. 26 (2001) 1660–1662.

[22] M. Abramowitz, I.A. Stegun, in: Handbook of Mathematical Functions, Dover, New York, 1965.

[23] M.J. Steel, T.P. White, C.M. de Sterke, R.C. McPhedran, L.C. Botten, Opt. Lett. 26 (2001) 488–490.

[24] M. Koshiba, K. Saitoh, IEEE Photon. Technol. Lett. 13 (2001) 1313–1315.